Electrolithographic Investigations of the Hydrophilic Channels in Nafion Membranes

Ju Chou,[†] Eric W. McFarland,[†] and Horia Metiu*[,‡]

Departments of Chemical Engineering, of Physics, and of Chemistry and Biochemistry, University of California, Santa Barbara, California 93106

Received: September 16, 2004; In Final Form: December 13, 2004

Nafion membranes are used as semisolid electrolytes in methanol and hydrogen fuel cells. The ion conduction takes place through those hydrophilic channels in the Nafion that can provide continuous pathways through the membrane. There is as yet limited information about the density, the size, and the shape of these channels. We have developed two electrochemical methods of visualizing the pore structure which involve the creation of metal lithographs using the membrane pores as templates. In the experiments, the membrane is supported on a flat solid surface on one side, and is in contact with an electrolyte on the other side. Using hydrogen-terminated n-doped Si(111), we deposited gold from an electrolyte containing a gold salt. The Au ions traverse the membrane through the pores, reach the silicon surface, and are spontaneously reduced. A metallic Au deposit is formed on the silicon surface, at the base of the hydrophilic channel. The Au deposits are imaged after the membrane is dissolved. Another method involves supporting the membrane on a Pt surface and depositing silver wires through the hydrophilic channels of the membrane. The scanning electron microscope pictures of these wires provide an image of the size and the shape of the hydrophilic channels.

I. Introduction

Nafion membranes are used as "electrolytes" to conduct protons in hydrogen and methanol fuel cells.[1,2] It is widely accepted that the material in a Nafion membrane self-organizes to form hydrophilic and hydrophobic domains. The hydrophobic regions consist primarily of Teflon, while the hydrophilic domains contain a mixture of sulfonic groups (present at the end of the side chains of the Teflon backbone), protons, water, and methanol.[3−9] The detailed morphology of the hydrophilic domains is important for several reasons. First, the proton mobility depends on the size of the hydrophilic channels. Second, since only the hydrophilic domains conduct protons, the membrane can function as an electrolyte in a fuel cell only if continuous hydrophilic channels cross the membrane. Finally, the morphology of the channels affects the degree of utilization of the electrocatalyst. The proton created by the Pt/Ru anode must travel through the hydrophilic channels in the membrane to react with oxygen, at the Pt cathode. Only a hydrophilic channel that has a Pt/Ru particle at one end continuously crosses the membrane, and one that has a Pt particle at the other end participates in electricity production. The catalytic particles that do not satisfy these conditions are wasted (see Figure 1). A method of fabrication that places the catalytic particles only at the ends of those hydrophilic channels that cross the membrane will achieve the most efficient catalyst loading.

Little is known about the morphology of the membrane channels,[10,11] and nothing, to our knowledge, is known about the morphology of those channels that *cross the membrane.* Scattering methods give the mean size of the hydrophilic domains,[12] and scanning methods probe only one face of the membrane.[13−15] The work presented here uses two experimental procedures to determine the number of channels crossing the membrane, as well as their size and shape.

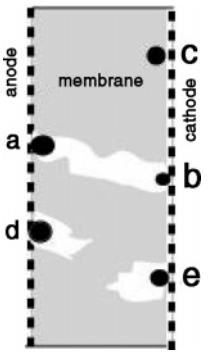

Figure 1. Schematic drawing of a polymeric membrane fuel cell. The dotted lines show the carbon cloth electrodes. The black circles are the catalyst particles. The hydrophobic domains are shown in gray, the hydrophilic ones in white. Only catalytic particles a and b contribute to the current in the cell; particles c−e are wasted. The figure ignores the existence of cross-linking between channels.

The idea is very simple. Consider a Nafion membrane supported on a flat solid surface on one side and in contact with an electrolyte solution on the other side (Figure 2). The metal ions can travel, from the electrolyte to the surface of the support, through the hydrophilic channels of the Nafion membrane.[16] If we choose the cations and the support appropriately, the cation reaching the solid surface is reduced spontaneously and forms a metal deposit at the place of contact between the hydrophilic channel and the support. Such deposits are formed only in a hydrophilic channel that crosses the membrane (to provide a continuous link between the electrolyte and the support). After deposition, we dissolve the membrane, image the metal deposits by AFM and SEM, and determine the surface composition by energy-dispersive spectroscopy (EDS). The metal deposits provide a footprint of the channels that cross the membrane, and their density (500−600 per μm^2) and their size (ranging from several nanometers to 100 nm) reflect those of the channels.

* To whom correspondence should be addressed. E-mail: metiu@chem.ucsb.edu.
[†] Department of Chemical Engineering.
[‡] Departments of Physics and of Chemistry and Biochemistry.

10.1021/jp0457848 CCC: $30.25
Published on Web 02/08/2005

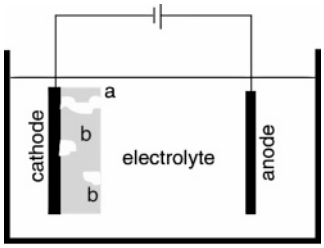

Figure 2. A schematic diagram of the experimental setup. The membrane (gray) is supported either on a Si electrode (black) or on a Pt film, and is submerged in an electrolyte. We show in white two hydrophilic channels: channel a traverses the membrane, and channel b does not. We either choose an electrolyte whose cation will deposit spontaneously on Si, when it comes in contact with it or perform electrochemistry to deposit a metal, on the Pt/Si electrode, through the membrane. In both cases, metal is deposited only through hydrophilic channels that cross the membrane.

In a second method of visualization, we use the support as cathode and deposit metal on it electrochemically. In this way, we grow metal "wires" in the channel. Dissolving the membrane, after deposition, allows us to visualize the wires and hence the shape and size of the channels.

II. Experiments

II.1. Spontaneous Deposition of Au through a Nafion Membrane. In these experiments we take advantage of the fact that a Si surface in contact with a solution containing Au cations will reduce the Au spontaneously (electroless deposition) to form metallic Au deposits on the surface.[17,18] We start our experiments by depositing a Nafion membrane on a Si surface. We use a Si(111) wafer (n-doped with phosphorus, resistivity 1−10 Ω/cm, International Wafer Service), washed for 5 min in acetone and then rinsed twice with distilled water in a sonicator to remove organic grease. Then, we immerse the Si surface in a buffered HF solution, for 2 min, to remove the oxide layer. After that, we wash the surface with distilled water. This procedure produces a hydrogen-terminated H−Si(111) surface.[19,20]

Nafion perfluorinated ion-exchange resin (5 wt % solution in a mixture of lower aliphatic alcohols and water, equivalent weight (polymer mass per mole of ion-exchange sites) 1100) was purchased from Aldrich. This solution was prepared from a Nafion 117 membrane (Dupont) with the molecular structure[3]

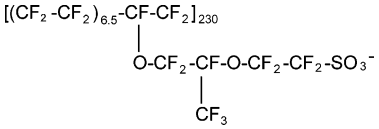

To form the membrane studied here, we dip the H−Si(111) surface into a Nafion solution for 20 s. Then we take the sample out and let the solvent evaporate, in contact with the atmosphere until the membrane appears dry. This leaves a Nafion membrane on the H−Si(111) surface.[15] The thickness of this membrane is about 2−3 μm, as measured by SEM. This method of preparation is different from that used when a fuel cell is made, and we expect our membrane to have properties different from those of membranes used commercially.

To deposit Au spontaneously, through the pores of the Nafion membrane, we bring the membrane into contact with a mixture of plating solution[17] (0.01 M $HAuCl_4$ + 0.5 M H_2SO_4) and concentrated HF (∼49%). The two solutions were mixed together in a volume ratio of 9:1, and 20 μL of mixture was placed on the top of the membrane (which is placed horizontally). The final composition of the solution with which the membrane is in contact is $HAuCl_4$ (0.009 M), H_2SO_4 (0.45 M), and HF (4.9%). The contact time between the membrane and the solution is approximately 2 min. After deposition, the samples are air-dried for several hours, and then the Nafion is removed by being dissolving into ethanol solution. The Au nanoparticles still remain on the surface, marking the position of the ion channels that traverse the membrane. The samples are air-dried again before imaging with SEM and AFM.

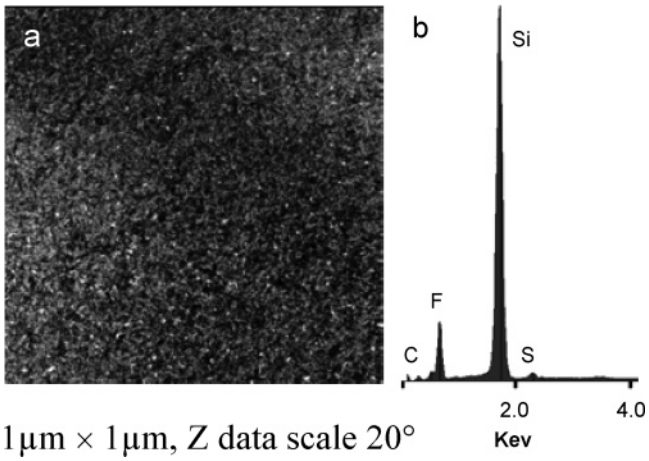

Figure 3. (a) AFM image and (b) energy-dispersive spectroscopy of the surface of a Nafion membrane formed on the Si(111)−H surface.

We compare the deposits formed on the Nafion-covered Si surface to those obtained, under identical conditions, on a Si surface without the membrane.

II.2. Electrochemical Deposition of Ag through a Nafion Membrane. We also visualize the channels that cross the membrane by electrodepositing Ag, through the hydrophilic channels of the membrane, on a conducting electrode and growing a Ag wire into the channel. The substrate is prepared from a Si(111) wafer with a native oxide washed for 5 min in acetone and then in distilled water. A Pt film, of 1000 Å thickness, is then deposited by electron beam evaporation. After that, a Nafion film is formed on top of the Pt layer, by using the procedure described above. The electrodeposition of silver, either through the membrane (Nafion/Pt/Si) or on it (Pt/Si), was performed at a constant potential of −2.0 V for 20 s, from a 0.05 M $AgNO_3$ solution in distilled water. The $HAuCl_4 \cdot 3H_2O$ (99.9%) and $AgNO_3$ used in these experiments were purchased from Sigma-Aldrich, and all solutions were prepared with deionized water.

II.3. Characterization of Nanoparticles and Nanofilms. To image the metal deposits, after membrane removal, we use a Digital Instruments DI 3000 atomic force microscope (Veeco, Santa Barbara), in a tapping mode, monitoring both the height and the phase image. The SEM images and the EDS spectra were obtained with a Philips XL-30 ESEM-FEG (ESEM stands for environmental scanning electron microscope and FEG for the field emission gun with which the ESEM is equipped). The EDS instrument is equipped with a PRISM Intrinsic Germanium detector manufactured by Princeton Gamma Technology. The energy-dispersive spectrum was taken from the same area as the SEM images.

III. Results

III.1. Nafion Membrane Formed on the H−Si(111) Surface. Figure 3 shows the AFM image of the Nafion-coated H−Si(111) surface prepared as described in the previous section. The picture indicates that a uniform Nafion film was formed on the silica surface. It is assumed that the bright features in

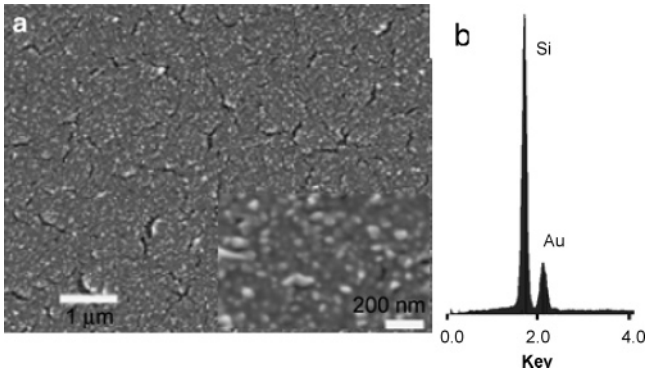

Figure 4. (a) Scanning electron micrograph and (b) energy-dispersive spectrum of a Au film deposited on the H−Si(111) surface by electroless deposition. The deposition time is 2 min. The scale bar is 200 nm in the inset image (high-resolution image). The thickness of the Au film is approximately 40−50 nm.

the image correspond to the hydrophilic domain reaching the surface and dark features show the hydrophobic domains.[15]

Energy-dispersive X-ray spectroscopy (Figure 3b) of the Nafion/H−Si(111) surface has peaks corresponding to sulfur, fluorine, and carbon, indicating that Nafion is present on the surface. The heights of the fluorine and sulfur peaks decrease gradually, indicating that the Nafion is decomposed by the electron beam and some of the fragments leave the surface. If the surface is not exposed to Nafion, only a Si peak is present in the ED spectrum (data not shown).

III.2. Spontaneous Au Deposition on the H−Si(111) Surface. Placing the H−Si(111) surface in contact with a 0.01 M $HAuCl_4$ + 0.5 M H_2SO_4 + 50% HF solution leads to the spontaneous formation of a continuous Au film (Figure 4a). This is consistent with previous work reported by Fujishima and co-workers.[17] The ED spectrum, taken during SEM imaging, has only a Si and a Au peak (Figure 4b). The surface of the Au film on H−Si(111) was also imaged by AFM, and a continuous Au film is observed in a 500 × 500 nm area. In the large-area scans we also observe cracks in the Au film. The presence of the cracks allows us to determine the thickness of the Au film (40−50 nm).

III.3. Au Deposition on the Nafion/H−Si(111) Surface. The Nafion-coated H−Si(111) surface was also exposed to the solution described above. The SEM image of the Au deposits, obtained without removing the Nafion membrane, is shown in Figure 5a, together with the ED spectrum (Figure 5b). In the presence of the Nafion, the image of the Au surface is blurry, suggesting that the Au nanoparticles are under the Nafion membrane. Au deposited through the Nafion membrane forms nanoparticles, not a continuous film. The ED spectrum shows the presence of S, F, Si, and Au, as expected. Since the electron beam removes the Nafion, the SEM image becomes clearer as the imaging process progresses and the peaks of F and S in EDS decrease.

Dipping the sample in an alcohol solution removes the Nafion from the surface. After drying the sample in the air for a while, we image the surface and do an elemental analysis by EDS. The image is now clearer, as we expect (Figure 5c), and the fluorine and the sulfur peaks disappear (Figure 5d). This indicates that the alcohol solution removes the Nafion from the surface, without removing the Au particles.

The AFM image of the Au/Si(111) surface obtained after the removal of the Nafion is shown in Figure 6b,d. Au forms disconnected particles on the surface. We believe that each particle is the footprint of a hydrophilic channel that crosses

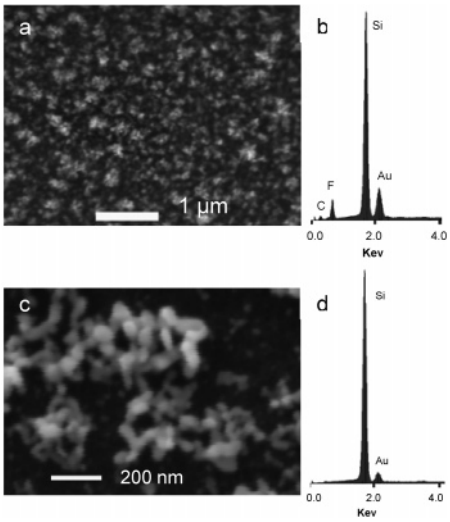

Figure 5. (a) Scanning electron micrograph and (b) energy-dispersive spectrum of Au deposited on the H−Si(111)/Nafion surface through Nafion, by electroless deposition. (c) and (d) are the image and spectrum taken after Nafion removal. The deposition time is 2 min.

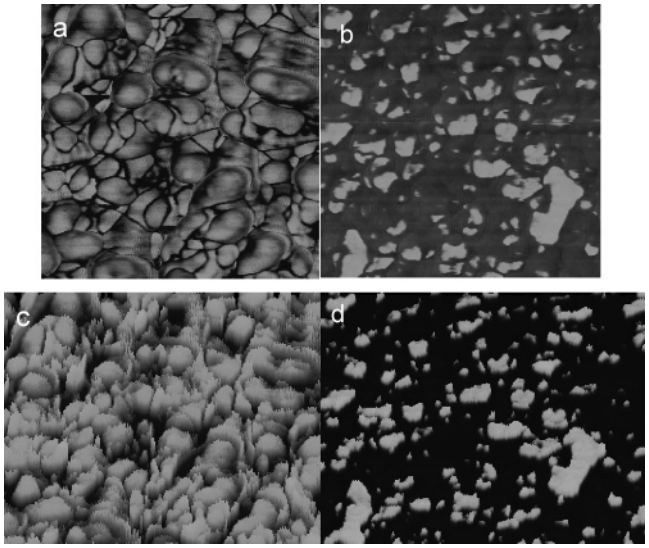

Figure 6. (a) and (c) are tapping mode AFM images of a Au continuous film deposited on the H−Si(111) surface without Nafion, by electroless deposition. (b) and (d) are images of Au nanoparticles deposited through Nafion, by the same electroless deposition, and both images were taken after the Nafion was dissolved. Images a and b show the phase and images c and d the height. The scales in all images are 500 nm × 500 nm, and the *z* data scale is 200°. The channel's diameter ranges from several nanometers 100 nm. There are about 150 ion channels in a 500 nm × 500 nm square area.

the membrane. The spontaneous deposition of Au on the Si surface, in the absence of Nafion, produces a continuous Au film (Figure 6a,c).

III.4. Electrochemical Deposition of Ag on Si(111)/Pt through the Nafion Membrane. To visualize the channels that cross the membrane, we have grown, electrochemically, Ag wires through them. To do this, we have supported the Nafion membrane on a Si(111) surface covered with a Pt film (which serves as an electrode). The membrane was immersed in a 0.05 M $AgNO_3$ solution, and Ag deposition was performed by using a three-electrode system with a Pt grid as an anode and an SCE as a reference at a constant potential of −2 V. The total deposition time is 20 s. After deposition, the Nafion was dissolved in alcohol solution, and the support was dried and imaged by SEM (Figure 7b). We believe that the wires seen in

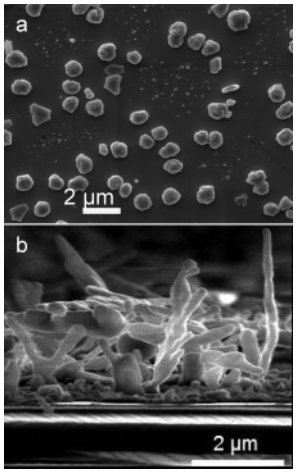

Figure 7. Scanning electron micrographs of (a) Ag deposition on the Pt/Si(111) surface and (b) the cross section of Ag deposition on the Nafion/Pt/Si(111) surface by electrochemical deposition at a constant potential of −2 V for 20 s. The Ag growth through Nafion shows the ion channels of Nafion.

the figure are images of the hydrophilic channels in Nafion. Note that some channels are straight, some are branched, and some are rather contorted. Only the channels which traverse the membrane can grow the metals. As we measured, the thickness of Nafion is about 2−3 μm, so some wires grow just inside the film, but long wires grow outside the Nafion membrane as well. The longest Ag nanowire seen in the SEM image (Figure 7b) is 3.7 μm, and this extends outside the membrane. The diameters of the wires range between several nanometers and 100 nm. These sizes are consistent with the dimensions observed in the AFM scans of the membrane.

Figure 7a shows an SEM image of a control experiment, in which Ag is deposited on the surface without Nafion. The two images contain the same amount of Ag, and the deposition conditions were identical. In the absence of Nafion, the Ag does not form a wire or grow dendrites: only Ag islands are observed in the SEM image.

IV. Discussion

To interpret the results of these experiments, we have made a number of assumptions that need clarification and further verification by future experiments. We have assumed that the ions travel only through the hydrophilic channels. We believe this to be a safe assumption. Simulations, as well as common sense, indicate that the largest driving force for channel formation is the energy gained by the solvation of the ions.[21] This leads to the dissociation of $-SO_3H$ and brings together the ions and the water. The Teflon chains are pushed out of this "solution" because their presence hinders both hydrogen bond formation and ion hydration. The energy to take a proton out of the hydrophilic domain and put it inside the region containing the Teflon chains is rather large, and therefore, ions travel overwhelmingly through the hydrophilic channels. This view is supported by the fact that the resulting metal deposits are spatially separated.

One might also be concerned with the possibility that, once a metallic deposit is formed, further metal deposition may take place on the sides of the existing deposit (in the electrochemical deposition method). This might make the wire grow thicker since not much energy is needed to deform the membrane to make room for this expansion. If this is true, then the thickness of the wire will exceed that of the hydrophilic channel in the membrane. This fear is unfounded for two reasons. First, the electric fields will be largest at the tip of the wire, due to its curvature. This field guides the ions toward the tip and causes the wire to grow there. Second, the energy of the system is lowered by solvation. Because of this, the ions will not travel along the side of the wire where the steric constraints prevent full solvation. It is true that if water binds strongly to the metal surface it will tend to form a monolayer on it, at the expense of the Nafion−metal contact. However, this is not enough for solvating the ions, which have the lowest energy when surrounded by a full solvation layer. Overall, it is more likely that the water and the ions will choose to stay in the hydrophilic channel, at the tip of the wire, rather than form a thick water-and-ion layer along the wire. Reliable simulations to clarify this issue would be very useful. At this time, we believe that the metal grows at the tip more readily than on the sides and that the size and the shape of the wire are representative of the size of the hydrophilic domain.

The formation of the metal deposits depends not only on the availability of the ions but also on the ability to nucleate a metal particle. It is therefore possible that some hydrophilic domains that cross the membrane are not visualized by this method, because the nucleation of the metal deposit did not take place. We have performed a few experiments with pulsed deposition, which creates different nucleation conditions, and found that the results were very similar to those obtained by continuous or spontaneous deposition.

In general, one should keep in mind that the size of the deposits and the amount of metal deposited reflect the kinetics of deposition. Channels having a low ionic conductivity will contain less metal than the ones having a high conductivity. This effect is enhanced by the fact that the growth of the wires is done in parallel and the channels compete for material: therefore, high-conductivity channels can slow the deposition in the low-conductivity channels. Similarly, in the case of spontaneous deposition, the rate of the surface reaction with silicon and the rate of ion diffusion through the channels control the size of the deposits. Superficially, one might think of this as a limitation in the accuracy of shape and size determination. However, we are interested in the size and the shape of the domains because they influence ion transport through the channels. These methods are even more interesting if they turn out to visualize ion transport through the channels.

It is possible that the area of contact between the hydrophilic channel and the support does not reflect the size of the channel in the bulk of the membrane. Crudely speaking, the shape of the channel at the interface is the result of the interplay between various interface and bulk free energies. If the free energy of the interface between the water−proton−sulfonic acid solution (forming the material in the hydrophilic channel) and the support is small, the area of contact will be large. In this case, the diameter of the channel will increase as it approaches the surface. The area of the footprint of the channel, visualized by these methods, is a property of the support and membrane, not only of the membrane alone. We are currently performing experiments with a membrane deposited on the carbon cloth used in making fuel cells and hope to perform further studies to explore how the size of the footprint depends on the support materials.

We need to emphasize that the hydrophilic channels seen in these measurements are larger than those measured by scattering methods. It is likely that this is due to the method of preparation of our membrane, which differs from that used for making fuel cells. Furthermore, during metal deposition, our membrane is in contact with a solution, and therefore, it has a higher water

content than other membranes; this will surely increase the size of the domains. Finally, it is possible that the presence of the Ag and Au ions, and the corresponding counterions, also affects the size of the domain. We hope to study in future work how the dimension of the hydrophilic domains and their density and distribution are affected by water loading, the method of preparation, and the nature of the solid support.

Finally, a perfect utilization of the electrocatalyst requires it to be deposited only in channels that cross the membrane and that each such channel should have an anodic catalyst at one end and a cathodic catalyst at the other. We are currently attempting to achieve this by deposition of the electrocatalyst electrochemically, in situ, after the carbon cloth electrodes and the membrane are mounted.

V. Conclusions

Electrochemical lithographic deposition and microscopy are employed to investigate the size, the shape, and the distribution of hydrophilic channels in the Nafion membrane. The electroless deposition of Au is used to deposit Au on the H−Si(111) surface free or covered with a Nafion membrane. In the absence of Nafion, a continuous Au film is formed spontaneously on the Si surface. When the surface is covered with Nafion, the Au cations traveling across the membrane form disconnected Au nanoparticles. These gold particles, imaged by AFM and SEM, and detected by EDS, are footprints of the hydrophilic channels that cross the membrane. The Ag nanowires formed in the membrane by electrochemical deposition of Ag are an image of the hydrophilic channels that cross the membrane. The number of ion channels is estimated to be 500−600 in a 1 μm $\times$ 1 μm square area, and their "diameter" ranges from several nanometers to 100 nm. The discovery of ion channels of Nafion and Au deposition through Nafion could potentially lower the cost of fuel cells because it is possible to deposit catalysts on the hydrophilic channels only.

Acknowledgment. The funding for this project was provided by a MURI grant from the Army Research Office. Characterization made use of MRL Central Facilities supported by the MRSEC Program of the National Science Foundation under Award No. DMR00-80034. We thank Alan Kleiman-Shwarsctein for preparing the Pt sample on Si wafers.

References and Notes

(1) Surampudi, S.; Narayanan, S. R.; Vamos, E.; Frank, H.; Halpert, G.; LaConti, A.; Kosek, J.; Prakash, G. K. Surya; Olah, G. A. *J. Power Sources* **1994**, *47*, 377−85.

(2) Chu, Y.-H.; Shul, Y. G.; Choi, W. C.; Woo, S. I.; Han, H.-S. *J. Power Sources* **2003**, *118*, 334−341.

(3) Haubold, H.-G.; Jungbluth, Th. V. H.; Hiller, P. *Electrochim. Acta* **2001**, *46*, 1559−1563.

(4) Paddison, S. J.; Paul, R.; Zawodzinski, T. A., Jr. *J. Electrochem. Soc.* **2000**, *147*, 617−626.

(5) Maruyama, J.; Inaba, M.; Katakura, K.; Ogumi, Z.; Takehara, Z. *J. Electroanal. Chem.* **1998,** *447*, 201−209.

(6) Shukla, A. K.; Raman, R. K. *Annu. Rev. Mater. Res.* **2003**, *33*, 155−168.

(7) Rice, C.; Tong, Y. Y,; Oldfield, E.; Wieckowski, A. *J. Phys. Chem. B* **2000**, *104*, 5803−5807.

(8) Lee, C. H.; Lee, C. W.; Kim, D. I.; Jung, D. H.; Kim, C. S.; Shin, D. R. *J. Power Sources* **2000**, *86*, 478−481.

(9) Arico, A. S.; Baglio, V.; Modica, E.; Di Blasi, A.; Antonucci, V. *Electrochem. Commun.* **2004**, *6*, 164−169.

(10) Paddison, S. J. *Annu. Rev. Mater. Res.* **2003**, *33*, 289−319.

(11) Kreuer, K.-D.; Paddison, S. J.; Spohr, E.; Schuster, M. *Chem. Rev.* **2004**, in press.

(12) Gebel G.; Lambard, J. *Macromolecules* **1997**, *30*, 7914−7920.

(13) James, P. J.; McMaster, T. J.; Newton, J. M.; Miles, M. J. *Polymer* **2000**, *41*, 4223−4231.

(14) James, P. J.; Antognozzi, M.; Tamayo, J.; McMaster, T. J.; Newton, J. M.; Miles, M. J. *Langmuir* **2001**, *17*, 349−360.

(15) Kanamura, K.; Morikawa, H.; Umegaki, T. *J. Electrochem. Soc.* **2003**, *150*, A193−A198.

(16) Huang, K.-L.; Holsen, T. M.; Chou, T.-C.; Selman, J. R. *Environ. Sci. Technol.* **2003**, *37*, 1992−1998.

(17) Nagahara, L. A.; Ohmori, T.; Hashimoto, K.; Fujishima, A. *J. Vac. Sci. Technol., A* **1993**, *11*, 763−767.

(18) Miyake, H.; Ye, S.; Osawa, M. *Electrochem. Commun.* **1997**, *13*, 5974−5978.

(19) Ziegler, J. C.; Reitzle, A.; Bunk, O.; Zegenhagen, J.; Kolb, D. M. *Electrochim. Acta* **2000**, *45*, 4599−4605.

(20) Hessel, H. E.; Feltz, A.; Reiter, M.; Memmert, U.; Behm, R. J. *Chem. Phys. Lett.* **1991**, *186*, 275−280.

(21) Blake, N.; Voth, G.; Metiu, H. Unpublished results.